JOURNAL OF GUIDANCE, CONTROL, AND DYNAMICS
Vol. 36, No. 5, September–October 2013

Engineering Notes

Magnetic Attitude Control of a Flexible Satellite

Everett J. Findlay*
University of Toronto, Toronto,
Ontario M3H 5T6, Canada
Anton de Ruiter†
Ryerson University, Toronto,
Ontario M5B 2K3, Canada
James R. Forbes‡
McGill University, Montreal,
Quebec H3A 0C3, Canada
Hugh H. T. Liu§ and Christopher J. Damaren¶
University of Toronto, Toronto,
Ontario M3H 5T6, Canada
and
James Lee**
Canadian Space Agency, Saint-Hubert,
Quebec J3Y 8Y9, Canada

DOI: 10.2514/1.57300

Nomenclature

$\mathbf{a}^{\times}$	=	skew-symmetric cross-product matrix associated with $\mathbf{a} \in \mathbb{R}^3$
$\mathbf{b}_b$	=	Earth's magnetic-field vector in $\mathcal{F}_b$ coordinates, T
d_{ij}	=	viscous damping constant for panel i about axis j, $\mathrm{N} \cdot \mathrm{m} \cdot \mathrm{s/rad}$
h_w	=	wheel bias momentum, $\mathrm{N} \cdot \mathrm{m} \cdot \mathrm{s}$
$\mathbf{h}_w$	=	wheel bias-momentum vector, $\mathrm{N} \cdot \mathrm{m} \cdot \mathrm{s}$
$\mathbf{J}_b$	=	moment-of-inertia matrix for spacecraft central body, $\mathrm{kg} \cdot \mathrm{m}^2$
$\mathbf{J}_r$	=	moment-of-inertia matrix for entire spacecraft in the undeformed state, $\mathrm{kg} \cdot \mathrm{m}^2$
k_{ij}	=	spring stiffness for panel i about axis j, $\mathrm{N} \cdot \mathrm{m/rad}$
$\tilde{\mathbf{M}}$	=	mass matrix for flexible spacecraft
$\mathbf{m}$	=	magnetic-torquer dipole vector, $\mathrm{A} \cdot \mathrm{m}^2$
T	=	orbital period, s
$\mathbf{u}_m$	=	desired control torque to be applied to a spacecraft by the magnetic torquers, $\mathrm{N} \cdot \mathrm{m}$
u_w	=	desired control torque to be applied to a spacecraft by the wheel, $\mathrm{N} \cdot \mathrm{m}$
$\delta\boldsymbol{\omega}$	=	angular velocity relative to an orbiting frame, rad/s
$[\epsilon, \epsilon_4]$	=	quaternion representation of attitude relative to an orbiting frame
θ_j^{ib}	=	ith panel rotation about axis j, rad
$\tilde{\boldsymbol{\theta}}^{ba}$	=	$[\theta_x^{ib}, \theta_y^{ib}]^T$, rad
$\boldsymbol{\tau}$	=	total applied control torque, $\mathrm{N} \cdot \mathrm{m}$
$\boldsymbol{\tau}_m$	=	magnetic torque, $\mathrm{N} \cdot \mathrm{m}$
$\boldsymbol{\omega}$	=	inertial angular velocity, rad/s
ω_o	=	orbital angular rate, rad/s
$\mathbf{1}$	=	identity matrix
$\mathbf{1}_n$	=	unit vector defined by $\{\mathbf{1}_n\}_i = \begin{cases} 0, & i \neq n \\ 1, & i = n \end{cases}$

Presented as Paper 2011-6706 at the 2011 Guidance, Navigation and Control Conference, Portland, Oregon, 8–11 August 2011; received 14 December 2011; revision received 5 December 2012; accepted for publication 12 January 2013; published online 2 July 2013.

*M.Sc. Candidate, Institute for Aerospace Studies, 4925 Dufferin Street. Student Member AIAA.

†Assistant Professor, Department of Aerospace Engineering, 350 Victoria Street. Senior Member AIAA.

‡Assistant Professor, Department of Mechanical Engineering and Centre for Intelligent Machines, 817 Sherbrooke Street West. Member AIAA.

§Associate Professor, Institute for Aerospace Studies, 4925 Dufferin Street. Senior Member AIAA.

¶Professor, Institute for Aerospace Studies, 4925 Dufferin Street. Associate Fellow AIAA.

**Research Scientist, Space Science and Technology, 6767 route de l'Aeroport. Member AIAA.

I. Introduction

THIS note presents a study on the attitude control of a flexible satellite using three mutually perpendicular magnetic torque rods (magnetorquers) and a single reaction wheel. The research is motivated by JC2Sat, a proposed satellite-formation-flying mission using differential drag as the means of formation control [1]. To increase or decrease the atmospheric drag for each satellite, pitch-attitude maneuvers are performed to increase or decrease the satellite frontal (drag) area. The purpose of the momentum wheel is to gyroscopically stabilize the pitch axis and perform rapid pitch maneuvers. Roll and yaw stabilization is provided by magnetic torquers. To make formation control using differential drag feasible, this type of satellite generally has relatively small mass and large drag panels (to increase the ballistic coefficient). This can result in significant satellite structural flexibility, which could degrade the performance of the attitude-control system. To the authors' best knowledge, simultaneous attitude control and vibration suppression using magnetic actuation has not been treated in the literature previously.

The motivation for the study presented in this note is to see whether it is possible to actively suppress structural vibrations when magnetic actuation is used as the means for attitude control. The answer to this question is not immediately obvious for two reasons. First, magnetic actuation has inherently low control authority. Second, spacecraft with magnetic control are instantaneously underactuated. This is due to the well-known fact that magnetic torquers can only generate torques perpendicular to the local Earth's magnetic-field vector [2]. It is the variation of the local Earth's magnetic field within an orbit that provides on-average controllability when magnetic actuation is used [3]. A recent survey outlines several methods used in magnetic attitude control [3]. The different methods can be grouped into linear and nonlinear approaches.

The most common method among the linear control-design techniques is to take advantage of the (quasi)-periodic nature of Earth's magnetic field. This involves using the linearized state-space model of the system and solving a periodic Riccati equation (PRE) to get an optimal time-periodic set of control gains. Using the periodic-control theory, it has been shown that the linearized closed-loop system is asymptotically stable [4]. A similar approach has also been used for disturbance-torque attenuation [5]. In [6], an infinite horizon, a finite horizon, and a time-invariant controller are proposed and compared. It is found for circular orbits that the finite horizon controller performs much better than the infinite horizon and time-invariant controllers. Another time-invariant controller was proposed in [7], which uses a constant gain matrix that approximates the solution to the PRE. It, however, does not guarantee asymptotic stability, unlike the time-varying solution.

Among the nonlinear control-design techniques, a number of works [8–10] again use the periodicity assumption of Earth's magnetic field and use Krasovskii–LaSalle-type arguments to prove local asymptotic stability. The resulting controllers have the challenges of being time varying. A different approach in [11,12], which does not make any periodicity assumptions, provides a time-invariant proportional–derivative-type control law. This has been done for both an inertially pointing [11] and Earth-pointing [12] satellites. A sufficient condition for stability in [11,12] is that the control gains must be less than an upper bound. However, there is no analytical way of determining the upper bound. As a consequence, numerical simulations must be performed to verify closed-loop stability. In [13], it is shown that, if a minimum level of an independent three-axis control system, such as reaction wheels, is used, the gain limitation in [11,12] can be removed. The methods in the works mentioned here only treat the magnetic attitude control of rigid spacecraft. To the authors' best knowledge, the only published work on using the magnetic attitude control of flexible satellites is [14], which is an extension of the work in [11,12]. Similar to [11,12], it is shown in [14] that, if the control gains are below some upper bound (which cannot be determined analytically), asymptotic stability is guaranteed even in the presence of perturbations from flexible appendages. It does not, however, attempt to actively suppress the flexible vibrations.

In this Note, we propose two controllers that perform simultaneous attitude control and active vibration suppression using magnetic actuation. The first controller is time invariant, and the second is periodic. Both controllers are based on the linear-quadratic-regulator (LQR) theory. The time-invariant controller commands a desired magnetic control torque. The control torque is implemented magnetically by projecting it onto the plane perpendicular to the local Earth's magnetic field. The second controller directly commands the magnetic-torquer dipole moment as the control input. Because of the approximate periodic nature of the local Earth's magnetic field as seen on orbit, the resulting controller is periodic. The periodic controller takes inspiration from those presented in [4,5]. A significant differentiating feature in this work from [4,5] is that, unlike in those papers, the flexible dynamics are explicitly incorporated into the control design. The advantage of the time-invariant controller over the periodic controller is that it has significantly less computational storage requirements.

II. Satellite Model

The type of satellite under consideration has large drag panels attached to the satellite body using tape springs. Tape springs provide a lightweight and simple deployment mechanism, but once deployed, can be highly flexible. For small deflections, the tape springs can be treated as torsion springs [15]. The satellite model is treated as a central body with rigid drag panels attached by torsion springs such that there is both flapping and torsional vibrations for both panels, as shown in Fig. 1. The flapping and torsional vibrations are about the x and y axes of the panel frames, with angles θ_x^{ib} and θ_y^{ib}, respectively, for panels $i = 1, 2$. The satellite is assumed to be in a circular orbit, and the commanded attitude is nominally nadir pointing, with commanded pitch maneuvers every half-orbit (see Sec. IV for more details). Attitude control is provided by three mutually perpendicular magnetic torquers and a single momentum wheel aligned with the satellite's pitch axis.

The full set of nonlinear equations of motion can be found in [16]. These equations are not used for the design of the control laws (the appropriate models are given in Sec. III.A), but they are used in Sec. IV for the numerical simulation of the closed-loop system.

III. Controller Design

Four controllers are compared. All are linear, two are time invariant, and two are periodic. The simplest is a time-invariant controller that neglects flexibility (it assumes the satellite to be rigid). The other, more complex time-invariant controller attempts to actively suppress the panel vibrations by using an observer to estimate the unmeasured panel states. Both have the advantage of only needing a single constant gain matrix stored onboard the satellite. The time-varying controllers take advantage of the roughly periodic nature of Earth's magnetic field to determine a periodic gain matrix. The drawback is that the large amount of onboard data storage required to save gain matrices over time may make the controller infeasible to implement. However, the periodic nature of the gains makes it possible to replace them using Fourier series approximations [17], greatly reducing the data-storage requirements. As for the time-invariant case, one of the periodic controllers neglects flexibility, and the other actively suppresses vibrations. The controllers will be referred to as the time-invariant rigid (TIR), time-invariant vibration suppression (TIVS), periodic rigid (PR), and periodic vibration suppression (PVS), respectively.

A. Linear Models Used for the Control Design

This section presents the linear state-space models used for each of the control-law designs.

It is assumed that both the attitude ϵ and angular velocity $\delta\boldsymbol{\omega}$, relative to the orbiting frame, are available as measurements. As explained in more detail in Sec. IV, the commanded attitude is piecewise constant relative to an orbiting frame, with changes occurring each half-orbit. Assuming a momentum management scheme for the wheel, the wheel bias momentum h_w will stay near the set point. The only possibly significant deviations of h_w occur during maneuvers. However, these maneuvers are short, and so the deviation of h_w is temporary. Therefore, for the purposes of the control design, it is assumed that h_w is constant.

1. Linear Model for the TIR Control Design

When flexibility is neglected, the linear model is given by a linearization of Euler's equation together with the quaternion kinematics about the nadir-pointing attitude [18]:

$$\dot{\mathbf{x}} = \underbrace{\begin{bmatrix} \mathbf{O} & \frac{1}{2}\cdot\mathbf{1} \\ \mathbf{J}_r^{-1}\mathbf{A}_{21} & \mathbf{J}_r^{-1}\mathbf{A}_{22} \end{bmatrix}}_{\mathbf{A}_R} \underbrace{\begin{bmatrix} \epsilon \\ \delta\boldsymbol{\omega} \end{bmatrix}}_{\mathbf{x}} + \underbrace{\begin{bmatrix} \mathbf{O} \\ \mathbf{J}_r^{-1}[\mathbf{1}_2 \quad \mathbf{1}] \end{bmatrix}}_{\mathbf{B}_{\mathrm{TIR}}} \underbrace{\begin{bmatrix} u_w \\ \mathbf{u}_m \end{bmatrix}}_{\mathbf{u}_{\mathrm{TI}}}$$

$$\mathbf{y} = \underbrace{\begin{bmatrix} \mathbf{1} & \mathbf{O} \\ \mathbf{O} & \mathbf{1} \end{bmatrix}}_{\mathbf{H}_R} \begin{bmatrix} \epsilon \\ \delta\boldsymbol{\omega} \end{bmatrix} \tag{1}$$

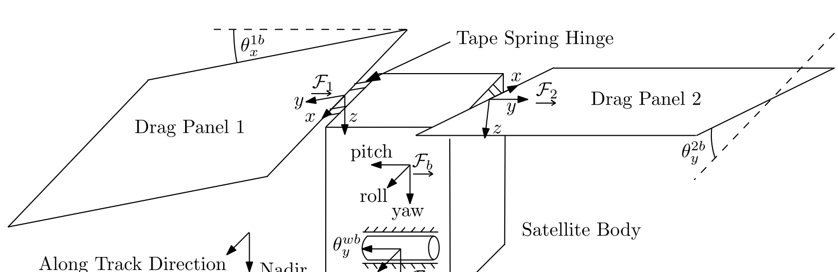

Fig. 1 Satellite showing hinge bending about x and y axes.

in which

$$\mathbf{A}_{21} = \mathrm{diag}\{a_z, 0, a_x\} \tag{2}$$

with $a_i = 2[h_w\omega_0 - (J_{ry} - J_{ri})\omega_0^2]$, and

$$\mathbf{A}_{22} = \begin{bmatrix} 0 & 0 & b \\ 0 & 0 & 0 \\ -b & 0 & 0 \end{bmatrix} \tag{3}$$

with $b = h_w + \omega_0(J_{rx} + J_{rz} - J_{ry})$. Note that J_{rx}, J_{ry}, and J_{rz} are the moments of inertia about the x, y, and z axes, respectively, assuming a principal axes frame for $\mathbf{J}_r$. The control-law design will provide laws for the desired torques u_w and $\mathbf{u}_m$. The actual wheel torque, $\boldsymbol{\tau}_w = [0 \quad u_w \quad 0]$, is the same as the desired torque. However, the magnetic torquers cannot, in general, deliver $\mathbf{u}_m$ because the actual torque $\boldsymbol{\tau}_m$ is always perpendicular to $\mathbf{b}_b$, as evidenced by [3]:

$$\boldsymbol{\tau}_m = \mathbf{m}^{\times}\mathbf{b}_b \tag{4}$$

Consequently, we project the desired magnetic torque $\mathbf{u}_m$ onto the plane perpendicular to the local Earth's magnetic field $\mathbf{b}_b$. The commanded magnetic-torquer dipole moment $\mathbf{m}$, which realizes this torque, is computed from [3]:

$$\mathbf{m} = \|\mathbf{b}_b\|^{-2}\mathbf{b}_b^{\times}\mathbf{u}_m \tag{5}$$

in which $\|\cdot\|$ denotes the Euclidean norm.

2. Linear Model for the PR Control Design

For the PR controller, we reuse the TIR model in Eq. (1), replacing the control input $\mathbf{u}_m$ with the magnetic-torquer dipole moment $\mathbf{m}$. Therefore, using Eq. (4), the linear PR model is the same as Eq. (1), with $\mathbf{B}_{\mathrm{TIR}}$ and $\mathbf{u}_{\mathrm{TI}}$ replaced by

$$\mathbf{B}_{\mathrm{PR}}(t) = \begin{bmatrix} \mathbf{O} \\ \mathbf{J}_r^{-1}[\mathbf{1}_2 - \hat{\mathbf{b}}_b^{\times}] \end{bmatrix}, \qquad \mathbf{u}_P = \begin{bmatrix} u_w \\ \hat{\mathbf{m}} \end{bmatrix} \tag{6}$$

in which $\hat{\mathbf{b}}_b = \mathbf{b}_b/\|\mathbf{b}_b\|$ and $\mathbf{m} = \|\mathbf{b}_b\|\hat{\mathbf{m}}$.

3. Linear Models for the TIVS and PVS Control Designs

For the TIVS and PVS control designs, the panel states are included, such that the state vector is $\mathbf{x}^T = [\boldsymbol{\varepsilon}^T\tilde{\boldsymbol{\theta}}^{1bT}\tilde{\boldsymbol{\theta}}^{2bT}\delta\boldsymbol{\omega}^T\dot{\tilde{\boldsymbol{\theta}}}^{1bT}\dot{\tilde{\boldsymbol{\theta}}}^{2bT}]$. The linear model used for the TIVS controller is

$$\dot{\mathbf{x}} = \underbrace{\begin{bmatrix} \mathbf{O} & \bar{\mathbf{A}}_{12} \\ \tilde{\mathbf{M}}^{-1}\bar{\mathbf{A}}_{21} & \tilde{\mathbf{M}}^{-1}\bar{\mathbf{A}}_{22} \end{bmatrix}}_{\mathbf{A}_{\mathrm{VS}}}\mathbf{x} + \underbrace{\begin{bmatrix} \mathbf{O} \\ \tilde{\mathbf{M}}^{-1}\begin{bmatrix} \mathbf{1}_2 & \mathbf{1} \\ \mathbf{O} & \end{bmatrix} \end{bmatrix}}_{\mathbf{B}_{\mathrm{TIVS}}}\mathbf{u}_{\mathrm{TI}}$$

$$\mathbf{y} = \underbrace{\begin{bmatrix} \mathbf{1} & \mathbf{O} & \mathbf{O} & \mathbf{O} \\ \mathbf{O} & \mathbf{O} & \mathbf{1} & \mathbf{O} \end{bmatrix}}_{\mathbf{H}_{\mathrm{VS}}}\mathbf{x} \tag{7}$$

in which $\bar{\mathbf{A}}_{12} = \mathrm{diag}\,\{0.5, 0.5, 0.5, 1, 1, 1, 1\}$, $\bar{\mathbf{A}}_{21} = \mathrm{diag}\{\mathbf{A}_{21}, -k_{1x}, -k_{1y}, -k_{2x}, -k_{2y}\}$, and $\bar{\mathbf{A}}_{22} = \mathrm{diag}\{\mathbf{A}_{22}, -d_{1x}, -d_{1y}, -d_{2x}, -d_{2y}\}$. Note that $\mathbf{A}_{21}$ and $\mathbf{A}_{22}$ are given in Eqs. (2) and (3), respectively.

The linear model for the PVS controller is the same as that for the TIVS model (7), with $\mathbf{B}_{\mathrm{TIVS}}$ replaced by

$$\mathbf{B}_{\mathrm{PVS}}(t) = \begin{bmatrix} \tilde{\mathbf{M}}^{-1}\begin{bmatrix} \mathbf{O} \\ \mathbf{1}_2 - \hat{\mathbf{b}}_b^{\times} \\ \mathbf{O} \end{bmatrix} \end{bmatrix} \tag{8}$$

and $\mathbf{u}_{\mathrm{TI}}$ replaced by u_P in Eq. (6).

B. Control Design

All four controllers (TIR, PR, TIVS, and PVS) are designed using the LQR framework [19], together with a state estimator based on a steady-state Kalman filter [19].

All systems in Sec. III.A take the form

$$\dot{\mathbf{x}} = \mathbf{A}\mathbf{x} + \mathbf{B}(t)\mathbf{u} \quad \mathbf{y} = \mathbf{H}\mathbf{x}$$

in which $\mathbf{B}$ is constant in the time-invariant case, and T periodic in the periodic case. The control laws take the form

$$\mathbf{u}(t) = -\mathbf{R}^{-1}\mathbf{B}^T(t)\mathbf{P}(t)\hat{\mathbf{x}}_e \tag{9}$$

$$\dot{\hat{\mathbf{x}}}_e = \mathbf{A}\hat{\mathbf{x}}_e + \mathbf{B}\boldsymbol{\tau} + \mathbf{L}(\mathbf{H}\hat{\mathbf{x}}_e - \mathbf{H}\mathbf{x}_e) \tag{10}$$

in which $\mathbf{L}$ is the filter gain, and $\mathbf{P}(t)$ is the symmetric positive semidefinite steady-state solution of the Riccati equation [20]

$$-\dot{\mathbf{P}}(t) = \mathbf{P}(t)\mathbf{A} + \mathbf{A}^T\mathbf{P}(t) - \mathbf{P}(t)\mathbf{B}(t)\mathbf{R}^{-1}\mathbf{B}^T(t)\mathbf{P}(t) + \mathbf{Q} \tag{11}$$

and $\mathbf{Q} \geq \mathbf{0}$ and $\mathbf{R} > \mathbf{0}$ are LQR weighting matrices. Note that $\mathbf{P}$ is constant in the time-invariant case, and T periodic in the periodic case. The vector $\mathbf{x}_e$ is the difference between the actual states, $\mathbf{x}$, and the desired ones, and $\hat{\mathbf{x}}_e$ is the estimate of $\mathbf{x}_e$. The distinction between $\mathbf{x}_e$ and $\mathbf{x}$ is made because, during the half of the orbit where the desired attitude is pitched forward (see Secs. II and IV), $\mathbf{x}_e$ and $\mathbf{x}$ are different. The filter gain chosen according to $\mathbf{L}$ is given by

$$\mathbf{L} = -\mathbf{P}_e\mathbf{H}^T\mathbf{Q}_v^{-1}$$

in which $\mathbf{P}_e > \mathbf{0}$ is the solution to the algebraic Riccati equation

$$\mathbf{P}_e\mathbf{A}^T + \mathbf{A}\mathbf{P}_e - \mathbf{P}_e\mathbf{H}^T\mathbf{Q}_v^{-1}\mathbf{H}\mathbf{P}_e + \mathbf{Q}_w = \mathbf{O}$$

in which $\mathbf{Q}_w > \mathbf{0}$ and $\mathbf{Q}_v > \mathbf{0}$ represent the covariances of the process noise and measurement noise, respectively, in a steady-state Kalman filter [19], but are tuned manually using simulations in Sec. IV.

If $(\mathbf{A}, \mathbf{B})$ are stabilizable and $(\mathbf{Q}^{1/2}, \mathbf{A})$ are detectable, and if $(\mathbf{H}, \mathbf{A})$ are observable, then the control by Eqs. (9) and (10) are stabilizing for the linearized system [19]. However, these stability guarantees are lost in the time-invariant cases when the control law is implemented via Eq. (4). That being said, there are several specific cases in the literature of magnetic attitude control using control implementations of the form (4), for which analytical stability proofs have been provided (see [1,11,12,14,21,22]). In the absence of an analytical stability proof for the time-invariant controllers in this Note, we provide a Monte Carlo-type analysis with numerical simulations in Sec. IV to demonstrate stability.

IV. Simulation

In this section, the proposed controllers are evaluated numerically using the exact nonlinear dynamic model for the JC2Sat satellites, which may be found in [16]. The numerical simulation and control parameters may also be found in [16].

As explained in Sec. I, JC2Sat is a proposed formation-flying mission using differential drag as the means for formation control. To mimic the steady-state formation maintenance, the commanded pitch angle is zero for half of each orbit, and 60 deg for the other half of each orbit. To reduce the sudden change in input to the control system, a smoothing function is used when the commanded pitch angle changes. The function spans 0.5% of the orbit (approximately 30 s). Saturation constraints for the magnetic torquers are enforced. Gaussian noise with a standard deviation of 0.5 deg is added to the attitude measurements. Arbitrary 5% adjustments are made to the satellite moment of inertia, the panel spring constants, as well as the applied control torque. This is to model the uncertainties in physical satellite parameters as well as actuator-output scaling and

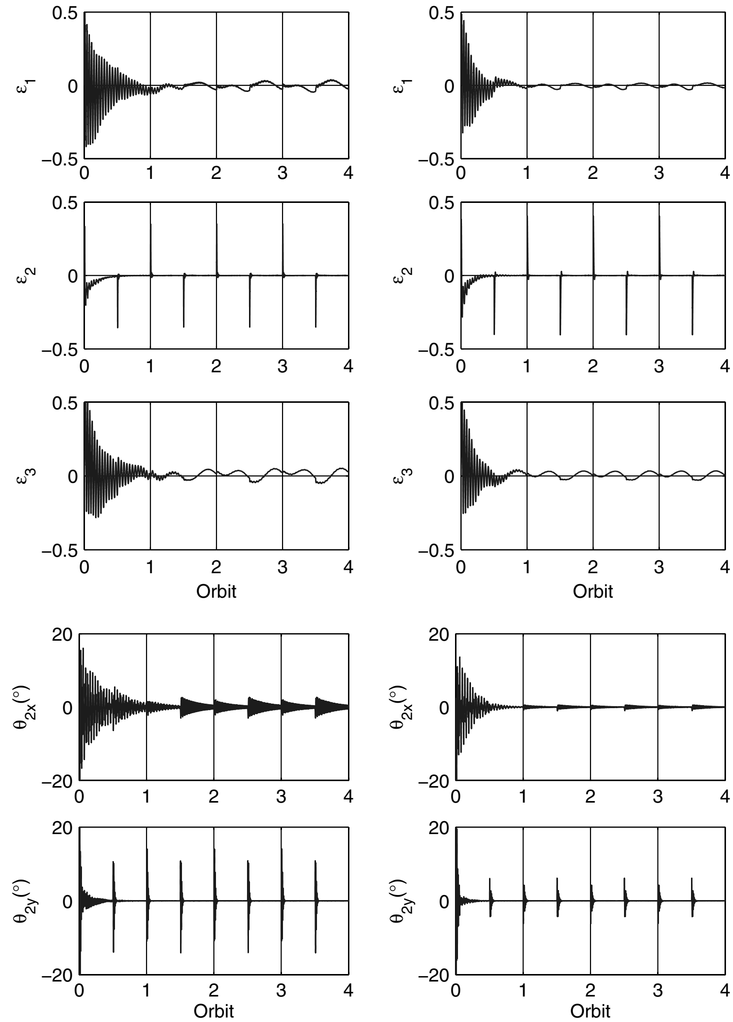

Fig. 2 Comparison of θ and $\tilde{\theta}^{2b}$ for the TIR (left) and TIVS (right) controllers.

misalignment errors. Gravity gradient and residual magnetic dipole-disturbance torques are included. The magnetic-field model used in both the simulation and in determining the PRE solutions is a tilted dipole model [2].

The 10th-order Fourier series is used to approximate $\mathbf{P}(t)$ in the periodic cases.

For each controller type, a set of Monte Carlo-type simulations is performed with randomly generated initial conditions. The purposes of this are twofold: first, to demonstrate the stability of the controllers, in particular the TIR and TIVS controllers for which there are no analytical guarantees, and second, to compare the performances of all four controllers across a broad range of initial conditions. The initial attitude error, angular velocity, and panel deflections are randomly generated from a zero-mean normal distribution, with standard deviations of 3 deg (Euler angle), 0.6 deg/s (angular velocity), and 7 deg (panel deflection), respectively. Forty simulations are performed for each controller type. It is important to note that, while the initial conditions for each controller type are randomly generated, each set of simulations (per controller type) is started with the same random-number-generator seed value. This means that each controller type has the same set of 40 initial conditions, making a comparison among them fair.

A typical set of simulation results (with nonzero initial conditions) is shown in Fig. 2, in which the TIR and TIVS controllers are compared for a four-orbit simulation. The results indicate that vibrations are mainly induced by nonzero initial conditions and the twice-per-orbit pitch maneuvers. It can be seen that the TIVS controller is able to stabilize the attitude slightly faster as well as have significantly smaller panel deflections. The results for the PR and PVS controllers are similar, and are therefore not shown. It can also be seen that the closed-loop system converges within one-and-a-half orbits. Therefore, all subsequent simulations are performed for two orbits.

A summary of the controller performances may be found in Tables 1 and 2. Both the mean and peak (worst case) performances across each set of 40 simulations are presented. First of all, it is clear from the peak-performance values that all controllers are stabilizing. As seen from both the mean and peak-performance values in Tables 1 and 2, the TIVS and PVS controllers (which actively suppress vibrations) consistently outperform the TIR and PR controllers (which neglect vibrations) in terms of both attitude regulation as well as vibration suppression. However, this comes at a cost of slightly increased magnetic-torquer activity, which is to be expected. This confirms it is indeed possible to actively suppress spacecraft vibrations using magnetic actuation. On the other hand, the periodic controllers, PR and PVS (which incorporate Earth's magnetic field in the control design), only slightly outperform the time-invariant

Table 1 Monte Carlo performance summary for all four controllers: mean

	TIR	PR	TIVS	PVS
$\boldsymbol{\theta}$ rms error, deg	1.20	1.03	0.779	0.707
$\boldsymbol{\omega}$ rms error, deg/s	0.0748	0.0664	0.0505	0.0452
$\tilde{\boldsymbol{\theta}}^{1b}$ rms, deg	0.476	0.468	0.260	0.247
$\tilde{\boldsymbol{\theta}}^{2b}$ rms, deg	1.01	0.994	0.502	0.474
Average $\Vert\mathbf{m}\Vert_1$, $\mathrm{A\cdot m^2}$	0.397	0.415	0.466	0.506
Average $\vert u_w\vert$, $\mathrm{N\cdot m}$	10.6×10^{-5}	10.5×10^{-5}	6.36×10^{-5}	6.46×10^{-5}

Table 2 Monte Carlo performance summary for all four controllers: peak

	TIR	PR	TIVS	PVS
$\boldsymbol{\theta}$ rms error, deg	1.70	1.60	1.19	1.10
$\boldsymbol{\omega}$ rms error, deg /s	0.132	0.121	0.0926	0.0844
$\tilde{\boldsymbol{\theta}}^{1b}$ rms, deg	0.693	0.756	0.492	0.474
$\tilde{\boldsymbol{\theta}}^{2b}$ rms, deg	1.47	1.64	0.947	0.907
Average $\|\mathbf{m}\|_1$, $\mathrm{A \cdot m^2}$	0.693	0.674	0.712	0.760
Average $\|u_w\|$, $\mathrm{N \cdot m}$	11.5×10^{-5}	11.6×10^{-5}	7.35×10^{-5}	7.45×10^{-5}

controllers, TIR and TIVS (which do not incorporate Earth's magnetic field in the control design). Given the increased computational requirements of storing periodic gains onboard, this suggests that use of the time-invariant controllers is sufficient for practical purposes.

As mentioned, one of the main causes of vibration is the twice-per-orbit pitch maneuvers. A possible approach to further reduce the induced vibrations is input shaping of the pitch command [23]. This has been demonstrated to be quite effective in other attitude-control configurations when used in conjunction with an active-vibration-suppression scheme [24].

V. Conclusions

Time-invariant and periodic controllers have been proposed for simultaneous attitude control and vibration suppression for a flexible bias-momentum spacecraft using magnetic actuators.

The time-invariant controller projects a stabilizing control torque onto the plane perpendicular to the local Earth's magnetic field for implementation by the magnetic torquers. By performing this projection, analytical stability guarantees are lost. However, stability is demonstrated by the Monte Carlo numerical simulation. The periodic controller directly provides the magnetic-torquer dipole moment as the control input. Analytical stability guarantees can be made in this case.

The performances of these two proposed controllers have been compared numerically with similar time-invariant and periodic controllers, which neglect the satellite flexibility. It has been shown that, despite the inherently low control authority and instantaneous underactuation with magnetic control, the proposed controllers do significantly reduce the induced vibrations and provide more accurate attitude control (compared to the controllers that neglect flexibility). It was found that the periodic controller performed only slightly better than the time-invariant controller. Therefore, the time-invariant controller is a very good candidate for simultaneous attitude control and vibration suppression to reduce onboard computational requirements.

Acknowledgment

Research work presented in this Note is sponsored by the Natural Sciences and Engineering Research Council of Canada (NSERC) Collaborative Research and Development Grants (CRDPJ 356619-2007) and the Canadian Space Agency partnership support program. The authors also thank the anonymous reviewers for their useful comments that helped to improve the Note.

References

[1] de Ruiter, A., "A Fault-Tolerant Magnetic Spin Stabilizing Controller for the JC2Sat-FF Mission," *Acta Astronautica*, Vol. 68, Nos. 1–2, 2011, pp. 160–171.
doi:10.1016/j.actaastro.2010.07.012

[2] Wertz, J. R., *Spacecraft Attitude Determination and Control*, Kluwer Academic Publishers, Dordrecht, The Netherlands, 1978, pp. 636, 782–785.

[3] Silani, E., and Lovera, M., "Magnetic Spacecraft Attitude Control: A Survey and Some New Results," *Control Engineering Practice*, Vol. 13, No. 3, 2005, pp. 357–371.
doi:10.1016/j.conengprac.2003.12.017

[4] Pittelkau, M., "Optimal Periodic Control for Spacecraft Pointing and Attitude Determination," *Journal of Guidance, Control, and Dynamics*, Vol. 16, No. 6, 1993, pp. 1078–1084.
doi:10.2514/3.21130

[5] Lovera, M., De Marchi, E., and Bittanti, S., "Periodic Attitude Control Techniques for Small Satellites with Magnetic Actuators," *IEEE Transactions on Control Systems Technology*, Vol. 10, No. 1, 2002, pp. 90–95.
doi:10.1109/87.974341

[6] Wisniewski, R., "Linear Time Varying Approach to Satellite Attitude Control Using Only Electromagnetic Actuation," *Journal of Guidance, Control, and Dynamics*, Vol. 23, No. 4, 2000, pp. 640–646.
doi:10.2514/2.4609

[7] Psiaki, M. L., "Magnetic Torquer Attitude Control via Asymptotic Periodic Linear Quadratic Regulation," *Journal of Guidance, Control, and Dynamics*, Vol. 24, No. 2, 2001, pp. 286–394.
doi:10.2514/2.4723

[8] Wisniewski, R., and Blanke, M., "Fully Magnetic Attitude Control for Spacecraft Subject to Gravity Gradient," *Automatica*, Vol. 35, No. 7, 1999, pp. 1201–1214.
doi:10.1016/S0005-1098(99)00021-7

[9] Damaren, C. J., "Comments on 'Fully Magnetic Attitude Control for Spacecraft Subject to Gravity Gradient'," *Automatica*, Vol. 38, No. 12, 2002, p. 2189.
doi:10.1016/S0005-1098(02)00146-2

[10] Arduini, C., and Baiocco, P., "Active Magnetic Damping Attitude Control for Gravity Gradient Stabilized Spacecraft," *Journal of Guidance, Control, and Dynamics*, Vol. 20, No. 1, 1997, pp. 117–122.
doi:10.2514/2.4003

[11] Lovera, M., and Astolfi, A., "Spacecraft Attitude Control Using Magnetic Actuators," *Automatica*, Vol. 40, No. 8, 2004, pp. 1405–1414.
doi:10.1016/j.automatica.2004.02.022

[12] Lovera, M., and Astolfi, A., "Global Magnetic Attitude Control of Spacecraft in the Presence of Gravity Gradient," *IEEE Transactions on Aerospace and Electronic Systems*, Vol. 42, No. 3, 2006, pp. 796–805.
doi:10.1109/TAES.2006.248214

[13] Damaren, C. J., "Hybrid Magnetic Attitude Control Gain Selection," *Journal of Aerospace Engineering*, Vol. 223, No. 8, 2009, pp. 1041–1047.
doi:10.1243/09544100JAERO641

[14] Schiavo, F., Lovera, M., and Astolfi, A., "Magnetic Attitude Control of Spacecraft with Flexible Appendages," *Proceedings of the 45th IEEE Conference of Decision and Control*, IEEE, San Diego, CA, 2006, pp. 1545–1550.

[15] Seffen, K. A., and You, Z., "Folding and Deployment of Curved Tape Springs," *International Journal of Mechanical Sciences*, Vol. 42, No. 10, 2000, pp. 2055–2073.
doi:10.1016/S0020-7403(99)00056-9

[16] Findlay, E., "Investigation of Active Vibration Suppression of a Flexible Satellite Using Magnetic Attitude Control," Master's Thesis, University of Toronto, Toronto, 2011.

[17] Boyce, W. E., and DiPrima, R. C., *Elementary Differential Equations and Boundary Value Problems*, Wiley, Hoboken, NJ, 1992, pp. 520–531.

[18] Hughes, P. C., *Spacecraft Attitude Dynamics*, 2nd ed., Dover, New York, 2004, pp. 31, 59.

[19] Crassidis, J. L., and Junkins, J. L., *Optimal Estimation of Dynamics Systems*, 2nd ed., CRC Press, Boca Raton, FL, 2011, pp. 176–177, 529–535.

[20] Bittanti, S., Laub, A., and Willems, J., *The Riccati Equation*, Springer-Verlag, New York, 1991, pp. 138–142.

[21] Avanzini, G., and Giulietti, F., "Magnetic Detumbling of Spacecraft," *Journal of Guidance, Control, and Dynamics*, Vol. 35, No. 4, 2012, pp. 1326–1334.
doi:10.2514/1.53074

[22] de Ruiter, A., "Magnetic Control of Dual-Spin and Bias-Momentum Spacecraft," *Journal of Guidance, Control, and Dynamics*, Vol. 35, No. 4, 2012, pp. 1158–1168.
doi:10.2514/1.55869

[23] Singer, N. C., and Seering, W. P., "Preshaping Command Inputs to Reduce System Vibration," *Transactions of the ASME Journal of Dynamic Systems, Measurement and Control*, Vol. 112, No. 1, March 1990, pp. 76–82.
doi:10.1115/1.2894142

[24] Song, G., and Agrawal, B. J., "Vibration Suppression of Flexible Spacecraft During Attitude Control," *Acta Astronautica*, Vol. 49, No. 2, 2001, pp. 73–83.
doi:10.1016/S0094-5765(00)00163-6